Spatial anisotropy and rotational invariance of critical hard squares

1994 J. Phys. A: Math. Gen. 27 5101

(http://iopscience.iop.org/0305-4470/27/15/011)

J. Phys. A: Math. Gen. 27 (1994) 5101–5119. Printed in the UK

Spatial anisotropy and rotational invariance of critical hard squares

Masafumi Fujimoto†

The Institute of Physical and Chemical Research (RIKEN), Wako, Saitama, 351-01, Japan

Received 22 March 1994, in final form 20 June 1994

Abstract. We develop a new method to analyse solvable models defined on a square lattice rotated through an arbitrary angle φ with respect to the coordinate axes. In the method we introduce auxiliary faces into a rotated system to relate it with an inhomogeneous one in the natural orientation $\varphi = 0$. The inhomogeneous system is investigated by commuting a transfer matrix argument. As an application of the method, we consider interacting hard squares at the critical point. We discuss relations between spatial anisotropy and rotational (or conformal) invariance of the model in calculations of finite-size properties.

1. Introduction

In principle, averaged properties (such as magnetization, pressure, etc) of a system can be calculated from its microscopic Hamiltonian within the framework of the statistical mechanics. Practically, however, these kinds of calculations are very complicated. We call a model solvable if a compact expression of its (per-site zero-field) free energy is obtainable without any approximations.

We have many two-dimensional solvable models [1–3]. It is known that there exists a hidden symmetry called the Yang–Baxter relation (or equation) in their solvability [1, 3, 4]. Draw a square lattice so that its rows and columns are parallel to the horizontal and vertical axes, respectively (figure 1(a)); we will use the term 'natural' to refer to this lattice orientation. Impose on it periodic boundary conditions in both directions (toroidal boundary conditions). Then, a parametrized solution to the Yang–Baxter equation yields a family of commuting row-to-row transfer matrices (RRTMs). Using an equation for commuting RRTMs, we can determine the explicit forms of their eigenvalues and hence the free energy.

If a square lattice is drawn diagonally (figure 1(b)), the geometry is convenient to consider relations between two-dimensional solvable models and solvable quantum spin chains [1, 4–7]. For example, when interactions of the 6-vertex model become extremely anisotropic, its diagonal-to-diagonal transfer matrix (DDTM) is related to the Hamiltonian of the XXZ-Heisenberg chain [6, 7]. Some authors [8] showed how to solve the 6-vertex model with the DDTM by the Bethe ansatz method. Recently, Litvin and Priezzhev (LP) [9] analysed the 6-vertex model on a square lattice rotated through an arbitrary angle φ with respect to the natural lattice orientation (figure 1(c)). LP derived the Bethe ansatz equation for general φ by the use of a random walk representation for configurations of the model.

† Present address: Department of Physics, Nara Medical University, Kashihara, Nara 634, Japan.

0305-4470/94/155101+19$19.50

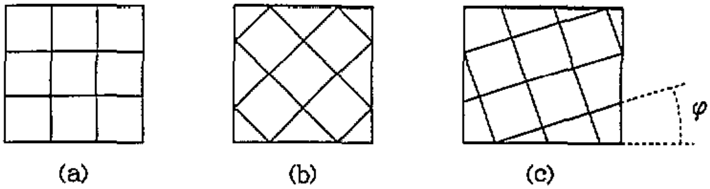

Figure 1. A square lattice (a) in the natural orientation, (b) drawn diagonally, and (c) rotated through φ with respect to the coordinate axes.

In the case of the ice model [10] the Bethe ansatz equation was solved numerically to find that several cases of φ give the same value of the per-site entropy $S = \left(\frac{3}{2}\right) \ln \left(\frac{4}{3}\right)$.

For conformally invariant models, LP indicated that the lattice rotation offers more interesting problems: The principle of scale invariance at the critical point is widely appreciated [11]. A critical model whose interactions are isotropic is expected to be invariant under a larger group, that of conformal transformations [12–14]. A conformal transformation is a point-to-point transformation which preserves angles but not necessarily distances. Locally, we can regard a conformal transformation as a combination of a dilatation (scale transformation), translation and rotation; and then, the length-rescaling factor, translation vector and rotation angles vary with position continuously. For lattice models it is difficult to carry out conformal transformations directly. Investigating their invariance under dilations, translations and rotations is helpful though the global transformations cannot be generalized to local ones automatically.

In two dimensions, it is convenient to introduce the complex coordinate: $z = x + \mathrm{i}y$. The conformal group is isomorphic to that of analytic functions. If we assume a conformally invariant model wrapped on a torus of size $l \times l'$ ($l' \gg l \gg 1$) [14, 15], it is shown that the free energy F must be of the form [16]

$$F = ll'f - (l'/l)(\pi c/6) + \cdots \tag{1.1}$$

where f is the per-site free energy. A universal number c called the conformal anomaly (or central charge) appears in the l'/l correction term; note that the l'/l correction term is invariant under scale transformations $l \to \alpha l$, $l' \to \alpha l'$. For various solvable models the value of the central charge has been determined in analyses for $\varphi = 0$ [17–22]. It is desirable to show invariance of the l'/l correction term under lattice rotations. Applying the argument of LP (or the Bethe ansatz methods in [17, 18]) to these problems is very involved, however. Alternative methods are required.

In this paper we propose a method to analyse solvable models on a square lattice rotated through an arbitrary angle φ with respect to the coordinate axes. Introducing auxiliary faces, we relate a rotated system to an inhomogeneous one in the natural orientation. Then, the inhomogeneous system is investigated by commuting transfer matrices argument. The method is quite general in order to be applicable to a wide class of solvable models. Here we consider interacting hard squares [23–25]. Finite-size properties of the model are calculated at the critical point. In the case of isotropic interactions we prove rotational invariance of the l'/l correction term in (1.1). When $\varphi = \pi/4$ and interactions are extremely anisotropic, we discuss relations between the hard-square model and one-dimensional quantum systems.

The format of the present paper is as follows. In section 2 a hard-square model is defined. In section 3 we explain a method to analyse the model on a rotated lattice. In section 4 we calculate eigenvalue spectrum of the transfer matrix at criticality. From the results in section 4, finite-size properties are investigated in section 5. Section 6 is devoted to a summary and discussion.

2. Critical hard hexagons and tricritical hard squares

When Baxter solved the hard-hexagon model, he considered a square lattice gas model with nearest-neighbour exclusion (thus 'hard squares') and next-nearest-neighbour interactions [1, 23–25]: There is an occupation number $\sigma_i (= 0, 1)$ at each site i on a square lattice; $\sigma_i = 0$ if the site i is empty; $\sigma_i = 1$ if the site i is occupied by a particle. The Boltzmann weight is assigned on each unit face depending on particle configurations around it. We denote by $W(a, b, c, d)$ the Boltzmann weight of a face with occupation numbers a, b, c, and d counterclockwise starting from the south-west (SW) corner. The corresponding Boltzmann weight is

$$W(a,b,c,d) = \begin{cases} m z^{(a+b+c+d)/4} \mathrm{e}^{Kac+Lbd} t^{-a+b-c+d} & \text{if} \quad ab = bc = cd = da = 0 \\ 0 & \text{otherwise} \end{cases} \tag{2.1}$$

where m is a normalization factor of the partition function and t is a parameter which cancels out of the partition function. The thermal equilibrium state of the model is determined for a given value of one-particle activity z and diagonal interactions K, L. In the thermodynamic (z, K, L) space, the hard-square model is solvable on a two-dimensional manifold defined by

$$z = (1 - \mathrm{e}^{-K})(1 - \mathrm{e}^{-L})/(\mathrm{e}^{K+L} - \mathrm{e}^{K} - \mathrm{e}^{L}) . \tag{2.2}$$

The manifold (2.2) consists of three disjoint sheets. Each sheet is divided into two regimes by a line of critical or tricritical points: the first sheet is in the region $K > 0$, $L < 0$. The hard-hexagon model is located at the $K \to 0$, $L \to -\infty$ limit on it. A line of critical points which is given by (2.2) and the equation

$$z^{-1/2}(1 - z\mathrm{e}^{K+L}) = [(1 + \sqrt{5})/2]^{-5/2} \tag{2.3a}$$

separates regime I from regime II; regime I is a disordered fluid regime, and regime II a triangular (3×1) ordered solid one [1, 23, 24]. The third sheet, which is in the region $K < 0$, $L > 0$, is divided into regimes V and VI by a critical line. Situations of regime V (respectively VI) differ from those of regime I (respectively II) in the interchange of K and L.

In the case of attractive diagonal interactions ($K, L > 0$) the manifold (2.2) corresponds to the second sheet, which is composed of regimes III and IV. In the (z, K, L) space regime III is a first-order transition surface separating a disordered fluid phase and square ($\sqrt{2} \times \sqrt{2}$) ordered solid ones [25, 26]. Regime IV is an analytic continuation of regime III beyond a line of tricritical points but lies in a square ordered solid phase; on the second sheet the tricritical line is located by the additional equation

$$z^{-1/2}(1 - z\mathrm{e}^{K+L}) = -[(1 + \sqrt{5})/2]^{-5/2} . \tag{2.3b}$$

Hereafter, we restrict ourselves to the critical line on the first sheet (critical hard hexagons) and the tricritical line on the second sheet (tricritical hard squares). On the two lines, after m and t are determined suitably, the Boltzmann weights around a face are parametrized in terms of the trigonometric functions as

$$\begin{aligned} \omega_1 &= W(0,0,0,0) = \sin(2\lambda + v)/\sin 2\lambda \\ \omega_2 &= W(1,0,0,0) = W(0,0,1,0) = \pm \sin v/[\sin\lambda \sin 2\lambda]^{1/2} \\ \omega_3 &= W(0,1,0,0) = W(0,0,0,1) = \sin(\lambda - v)/\sin\lambda \\ \omega_4 &= W(1,0,1,0) = \sin(2\lambda - v)/\sin 2\lambda \\ \omega_5 &= W(0,1,0,1) = \sin(\lambda + v)/\sin\lambda \end{aligned} \tag{2.4}$$

where the crossing parameter $\lambda = \pi/5$; the spectral parameter v, which represents spatial anisotropy, is in the interval $-\lambda < v < 0$ for critical hard hexagons, and $0 < v < \lambda$ for tricritical hard squares [1, 23, 24].

In analyses we use the following properties satisfied by the face weights W [1, 3, 4].
(i) The Yang–Baxter relation

$$\sum_c W(a,b,c,a''|v)W(a'',c,b',a'|v')W''(c,b,b'',b'|v'')$$
$$= \sum_c W(a'',a,c,a'|v'')W(a,b,b'',c|v')W(c,b'',b',a'|v) \tag{2.5}$$

for all $a, a', a'', b, b', b'' = \pm 1$ with $v + v'' = v'$,
(ii) the standard initial condition

$$W(a,b,c,d|0) = \delta(a,c) \tag{2.6}$$

and
(iii) crossing symmetry

$$W(a,b,c,d|\lambda - v) = \left(\pm\sqrt{\frac{\sin\lambda}{\sin 2\lambda}}\right)^{a-b+c-d} W(b,a,d,c|v)\,. \tag{2.7}$$

The crossing symmetry shows that replacing the parameter v by $\lambda - v$ in (2.4) is equivalent to rotating the lattice through $\pi/2$. From (2.6) and (2.7) it is found that

$$W(a,b,c,d|\lambda) = \left(\pm\sqrt{\frac{\sin\lambda}{\sin 2\lambda}}\right)^{a-b+c-d} \delta(b,d)\,. \tag{2.6$'$}$$

3. Auxiliary faces method

In this section we explain a method for solving the hard-square model on a rotated lattice. Introducing auxiliary faces, we relate a rotated system to an inhomogeneous one in the natural orientation. Then, the inhomogeneous system is analysed by commuting transfer matrices argument.

We start with defining an inhomogeneous hard-square model. Suppose a square lattice of $M + N$ columns and $M' + N'$ rows ($M = lm$, $N = ln$, $M' = l'm$, $N' = l'n$) in the natural orientation, and impose on it toroidal boundary conditions. It is also assumed that v can vary from face to face. By v_{ij} we denote the value of v for the face whose south-west (SW) corner is the site (i, j). Set the v_{ij} to be

$$v_{ij} = \begin{cases} 0 & \text{for} \quad 0 \leqslant i \leqslant m-1,\ 0 \leqslant j \leqslant n-1 \pmod{m+n} \\ u_0 & \text{for} \quad m \leqslant i \leqslant m+n-1,\ 0 \leqslant j \leqslant n-1 \pmod{m+n} \\ \lambda - u_0 & \text{for} \quad 0 \leqslant i \leqslant m-1,\ n \leqslant j \leqslant m+n-1 \pmod{m+n} \\ \lambda & \text{for} \quad m \leqslant i \leqslant m+n-1,\ n \leqslant j \leqslant m+n-1 \pmod{m+n} \end{cases} \tag{3.1}$$

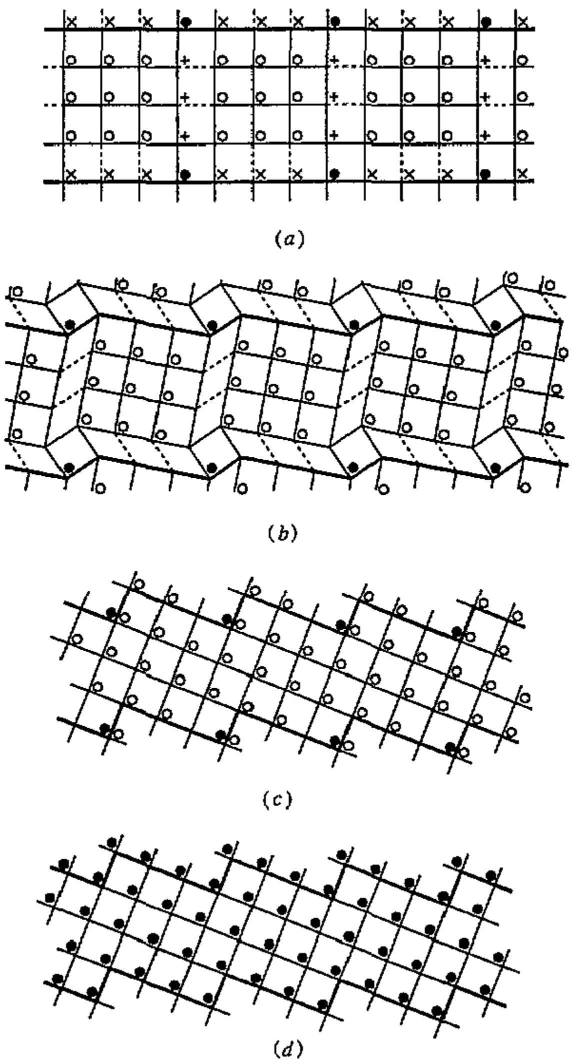

Figure 2. (*a*) Inhomogeneous system (3.1). Faces $v = 0$ (respectively u_0, $\lambda - u_0$, λ) are shown by $\times$ (respectively $\bullet$, $\circ$, $+$). (*b*) Shearing auxiliary faces $v = 0$ and λ, we deform the lattice into a rotated one. (*c*) The rotated lattice is composed of two kinds of faces $v = u_0$ and $\lambda - u_0$. (*d*) Using the crossing symmetry, we find the rotated model. In the rotated model $\mathbf{V}(u_0)$ is a transfer matrix between two zigzag-walls, which is represented by a full line.

where $0 < u_0 < \lambda$ for tricritical hard squares, and $-\lambda < u_0 < 0$ for critical hard hexagons (figure 2(*a*)). Faces with $v_{ij} = 0$ and λ are auxiliary ones. On each auxiliary face $v_{ij} = 0$ (respectively λ) occupation numbers of the SW, NE (respectively NW, SE) corners are always the same because of the standard initial condition (2.6) (respectively (2.6′)). Shearing auxiliary faces (figure 2(*b*)), we can continuously deform the lattice into a rotated one whose rotation angle φ is given by

$$\tan\varphi = m/n\,. \tag{3.2}$$

The rotated system consists of faces $v_{ij} = u_0$ and $\lambda - u_0$ (figure 2(*c*)). We note that the orientation of faces $v_{ij} = u_0$ is different from that of faces $v_{ij} = \lambda - u_0$ in the $\pi/2$-rotation. We use the crossing symmetry (2.7) for faces $v_{ij} = \lambda - u_0$. Then it is found that the inhomogeneous system (3.1) is equivalent to the hard-square model with $v = u_0$ rotated through φ with respect to the natural orientation (figure 2(*d*)). We can analyse the hard-square model rotated through φ by considering the inhomogeneous system (3.1).

The inhomogeneous system (3.1) is investigated by commuting transfer matrices argument. Let $\sigma = \{\sigma_1, \sigma_2, \ldots, \sigma_{M+N}\}$ and $\sigma' = \{\sigma'_1, \sigma'_2, \ldots, \sigma'_{M+N}\}$ are particle configurations of two successive rows with periodic boundary conditions. A one-parameter family of RRTMs is defined by elements as

$$[\mathbf{T}(u)]_{\sigma,\sigma'} = \left[-\frac{\sin(2\lambda+u)\sin\lambda}{\sin(2\lambda-u)\sin(\lambda+u)}\right]^M \left[-\frac{\sin(2\lambda+u+u_0)\sin\lambda}{\sin(2\lambda-u-u_0)\sin(\lambda+u+u_0)}\right]^N \times \prod_{i=0}^{l-1}\left[\prod_{j=i(m+n)}^{i(m+n)+m-1} W\left(\sigma_{j+1}, \sigma_{j+2}, \sigma'_{j+2}, \sigma'_{j+1}|u\right) \times \prod_{k=i(m+n)+m}^{(i+1)(m+n)-1} W\left(\sigma_{k+1}, \sigma_{k+2}, \sigma'_{k+2}, \sigma'_{k+1}|u+u_0\right)\right]. \tag{3.3}$$

From the same derivation of (3.3) in [24], we get a matrix equation for $\mathbf{T}(u)$ [27]:

$$\mathbf{T}(u)\mathbf{T}(u+\lambda) = \mathbf{I} + \mathbf{T}(u+3\lambda) \tag{3.4}$$

where $\mathbf{I}$ is the identity matrix. The Yang–Baxter relation (2.5) shows that, for all complex numbers u, u', $\mathbf{T}(u)$ and $\mathbf{T}(u')$ commute with each other, being simultaneously diagonalized. We denote the eigenvalues of $\mathbf{T}(u)$ by $T(u)$. It follows from (3.4) that each eigenvalue $T(u)$ satisfies the functional equation (or inversion identity)

$$T(u)T(u+\lambda) = 1 + T(u+3\lambda). \tag{3.5}$$

From the parametrization (2.4) we find the periodicity relation

$$T(u+\pi) = T(u). \tag{3.6}$$

Detailed analysis shows that the eigenvalue $T(u)$ must be of the form [20, 24]

$$T(u) = \left[-\frac{\sin(2\lambda+u)\sin\lambda}{\sin(2\lambda-u)\sin(\lambda+u)}\right]^M \left[-\frac{\sin(2\lambda+u+u_0)\sin\lambda}{\sin(2\lambda-u-u_0)\sin(\lambda+u+u_0)}\right]^N \times R\prod_{j=1}^{M+N}\sin(u-u_j) \tag{3.7a}$$

$$\sum_{j=1}^{M+N} u_j = 3(M+N)\lambda + k\pi \tag{3.7b}$$

where R is a constant, and k an integer. The zeros u_j are determined by substituting (3.7*a*) into (3.5), and then by solving (3.5) with (3.7*b*). Using a solution u_j in (3.7*a*), we find an expression for $T(u)$. There are many eigenvalues $T(u)$, corresponding to different solutions u_j.

After the eigenvalues $T(u)$ are calculated, we can get the necessary information to analyse the inhomogeneous system (3.1) and hence the rotated system by letting $u = 0$ and $\lambda - u_0$. For example, the partition function of the rotated system is given by

$$\begin{aligned}\Xi &= \mathrm{Tr}\big[\mathbf{V}(u_0)^{l'}\big] = \sum_j \big[V_j(u_0)^{l'}\big] \\ &= V_1(u_0)^{l'}\left[1 + \frac{V_2(u_0)^{l'}}{V_1(u_0)^{l'}} + \frac{V_3(u_0)^{l'}}{V_1(u_0)^{l'}} + \cdots\right]\end{aligned} \tag{3.8a}$$

$$\mathbf{V}(u_0) = \mathbf{T}(0)^n \mathbf{T}(\lambda - u_0)^m \tag{3.8b}$$

$$V_j(u_0) = T_j(0)^n T_j(\lambda - u_0)^m \qquad j = 1, 2, 3, \ldots \tag{3.8c}$$

where $T_j(u)$ (or $V_j(u)$) is the jth eigenvalue of $\mathbf{T}(u)$ (or $\mathbf{V}(u)$) in decreasing order of magnitude. In the rotated system, $\mathbf{V}(u_0)$ corresponds to a transfer matrix between two zigzag-walls, as shown in figure 2(d). The zigzag-wall transfer matrix reduces to the RRTM and DDTM when $m/n = 0$ and 1, respectively.

4. Finite-size corrections

Following the programs given in section 3, we analyse the rotated hard-square model. In this section, when l becomes large with m and n fixed to be constants, we calculate the asymptotic behaviour of the eigenvalues $T(u)$. In next section, substituting calculated eigenvalues into (3.8), we discuss finite-size properties of the rotated model from the viewpoint of the conformal field theory.

At the first place we briefly summarize predictions gained from the assumption of conformal invariance at criticality: two-dimensional critical models are classified into universality classes according to the central charge c of the Virasoro algebra, which is connected with the conformal invariance at the critical point [12–14]. There exists a sequence of universality classes of systems with unitarity [14, 28], where the central charge is given by

$$c = 1 - 6/m(m-1) \tag{4.1}$$

with $m = 4, 5, 6, \ldots$; tricritical hard squares corresponds to the case $m = 5$, and critical hard hexagons $m = 6$. For each value of c in (4.1) possible scaling dimensions x, which are power-law exponents for correlation functions of various scaling fields, are given by the conformal weights $(h, \bar{h})$ in the Kac table [14, 28, 29] as

$$x = h + \bar{h}\,. \tag{4.2}$$

If we suppose a conformally invariant model on a torus of $l \times l'$ [14, 15], the partition function is represented as

$$Z \sim \exp(-ll'f) Z_c(q) \tag{4.3a}$$

with

$$q = \exp 2\pi \mathrm{i}\tau \qquad \tau = \mathrm{i}l'/l \tag{4.3b}$$

where f is the per-site free energy and the finite-size correction $Z_c(q)$ is a universal term. By $\chi_h(q)$ we denote a character of a representation of the Virasoro algebra characterized by a highest weight h. Then $Z_c(q)$ is written as

$$Z_c(q) = \sum_{h,\bar{h}} N_{h,\bar{h}} \chi_h(q) \chi_{\bar{h}}(\bar{q}) . \tag{4.4}$$

The multiplicity factors $N_{h,\bar{h}}$ are determined by requiring that $Z_c(q)$ must be invariant under transformations of the modular group.

In the case of tricritical hard squares, we get

$$Z_c^{(\mathrm{sq})}(q) = |\chi_0(q)|^2 + |\chi_{3/80}(q)|^2 + |\chi_{1/10}(q)|^2 + |\chi_{7/16}(q)|^2 + |\chi_{3/5}(q)|^2 + |\chi_{3/2}(q)|^2 . \tag{4.5}$$

To compare (4.3) and (4.5) with the transfer matrix analysis (3.8), we assume that $l' \gg l \gg 1$, and expand the RHS of (4.5) as

$$\begin{aligned} Z_c^{(\mathrm{sq})}(q) \sim (q\bar{q})^{-7/240}\big[1 + (q\bar{q})^{3/80} + (q\bar{q})^{1/10} + (q\bar{q})^{7/16} + \big(q^{3/80}\bar{q}^{83/80} + q^{83/80}\bar{q}^{3/80}\big) \\ + (q\bar{q})^{3/5} + \cdots\big] . \end{aligned} \tag{4.6}$$

Substituting (4.6) into (4.3), and taking logarithms of both sides of (4.3), we find that the leading terms reduce to (1.1) with $c = \frac{7}{10}$.

Similarly, for critical hard hexagons, it is found that

$$Z_c^{(\mathrm{hx})}(q) = |\chi_0(q) + \chi_3(q)|^2 + |\chi_{2/5}(q) + \chi_{7/5}(q)|^2 + 2|\chi_{1/15}(q)|^2 + 2|\chi_{2/3}(q)|^2 \tag{4.7}$$

Expanding (4.7) into a power series of q, we get

$$\begin{aligned} Z_c^{(\mathrm{hx})}(q) \sim (q\bar{q})^{-1/30}\big[1 + 2(q\bar{q})^{1/15} + (q\bar{q})^{2/5} + 2(q^{1/15}\bar{q}^{16/15} + q^{16/15}\bar{q}^{1/15}) \\ + 2(q\bar{q})^{2/3} + 2(q^{2/5}\bar{q}^{7/5} + q^{7/5}\bar{q}^{2/5}) + \cdots\big] . \end{aligned} \tag{4.8}$$

The leading behaviour in the RHS of (4.8) shows that $c = \frac{4}{5}$.

4.1. Tricritical hard squares

Analytic calculations for critical models were very cumbersome [17, 18]. Recently, Klümper and Pearce developed a new approach to these problems [19–22]. They applied it to several solvable models to determine the central charge c and scaling dimensions x. For tricritical hard squares and critical hard hexagons these were done in [20] (KP); see also [19]. We use the arguments in KP to find asymptotic behaviour of $T(u)$ as $l \to \infty$. In this subsection we deal with tricritical hard squares, and in next subsection critical hard hexagons. Calculations are somewhat indirect. We obtain $T(u)$ without determining the zeros u_j explicitly. The inversion identity (3.5) is solved by the use of special values of Rogers dilogarithms.

For tricritical hard squares we suppose that $0 < u_0 < \lambda$, and that $M + N \equiv 0 \pmod 2$. In the complex u plane our attention is restricted to the strip $0 < \mathrm{Re}(u) < \lambda - u_0$. We calculate the largest eigenvalues there. The bulk behaviour of $T(u)$ is determined first. The parametrization (2.4) corresponds to the $x \to -1$ limit of (3.11) in [24]. When the transfer matrix is defined by (3.3) with the face weights (2.4) replaced by (3.11) in [24], we denote it by $\mathbf{T}(u; x)$, and its eigenvalues by $T(u; x)$. To find the largest eigenvalues $T(u; x)$ in the strip $0 < \mathrm{Re}(u) < \lambda - u_0$, we repeat almost the same argument as [27] in the $l \to \infty$ limit with m and n fixed to be constants. From the calculated eigenvalue $T(u; x)$, the bulk behaviour of $T(u)$ is estimated as

$$\lim_{l\to\infty} T(u)^{1/l} = \lim_{x\to-1}\lim_{l\to\infty} T(u;x)^{1/l} = \begin{cases} 1 & \text{for } u \text{ in strip 1} \\ Z(u) & \text{for } u \text{ in strip 2} \end{cases} \tag{4.9}$$

where

$$Z(u) = \left[\mathrm{i}\cot(5u/2)\right]^m \{\mathrm{i}\cot[5(u+u_0)/2]\}^n \tag{4.10}$$

and strips 1 and 2 are defined by

$$\begin{aligned} &\text{strip 1:} \qquad -\pi/10 < \mathrm{Re}(u) < 3\pi/10 - u_0 \\ &\text{strip 2:} \qquad 3\pi/10 < \mathrm{Re}(u) < 9\pi/10 - u_0\,. \end{aligned} \tag{4.11}$$

Secondly we derive integral equations for finite-size corrections. To the largest eigenvalue in $0 < \mathrm{Re}(u) < \lambda - u_0$, denoted by $T_1(u)$, the argument in section 2.1 of KP is applied with some modifications. Numerical analyses for finite-size systems show that (*a*) for sufficient large l and in a periodic strip $0 < \mathrm{Re}(u) < \pi$, the zeros u_j are in $3\pi/10 - u_0 < \mathrm{Re}(u) < 3\pi/10$ or $9\pi/10 - u_0 < \mathrm{Re}(u) < 9\pi/10$, and that (*b*) the distances of the furthest zeros from the real axis grow as $\ln l$. Though we cannot prove (*a*) and (*b*) rigorously, we are certain of the properties. In the $\mathrm{Im}(u) \to \pm\infty$ limit with the system size l fixed to be a constant, (3.5) becomes

$$t^2 = 1 + t \tag{4.12a}$$

with

$$t = \lim_{\mathrm{Im}(u)\to\infty} T(u) = \lim_{\mathrm{Im}(u)\to-\infty} T(u)\,. \tag{4.12b}$$

It follows that

$$t = \frac{(1+\sqrt{5})}{2} \qquad \text{or} \qquad \frac{(1-\sqrt{5})}{2}\,. \tag{4.12c}$$

From numerical results we find that (*c*) $t = (1+\sqrt{5})/2$ for $T_1(u)$.

Using (4.9), we define finite-size corrections of $T_1(u)$ in strips 1 and 2 by

$$T_1(u) = \begin{cases} 1\, l_1(u) & \text{for } u \text{ in strip 1} \\ Z(u)^l\, l_2(u) & \text{for } u \text{ in strip 2}\,. \end{cases} \tag{4.13}$$

Substituting (4.13) into (3.5), we get

$$\begin{aligned} l_1(u)l_1(u+\lambda) &= p_2(u) \qquad -\pi/10 < \mathrm{Re}(u) < \pi/10 - u_0 \\ l_2(u)l_2(u+\lambda) &= p_1(u) \qquad 3\pi/10 < \mathrm{Re}(u) < 7\pi/10 - u_0 \end{aligned} \tag{4.14}$$

where

$$
\begin{aligned}
p_1(u) &= 1 + T_1(u - 2\lambda) \qquad 3\pi/10 < \mathrm{Re}(u) < 7\pi/10 - u_0 \\
p_2(u) &= 1 + T_1(u + 3\lambda) \qquad -\pi/10 < \mathrm{Re}(u) < \pi/10 - u_0 .
\end{aligned}
\tag{4.15}
$$

In their respective strips, $l_1(u)$ and $l_2(u)$ are analytic. The property (a) shows that $l_1(u)$ (or $l_2(u)$) is non-zero in strip 1 (or 2), and (c) that the logarithms of $l_1(u)$ and $l_2(u)$ tend to constants as $\mathrm{Im}(u) \to \pm\infty$. Therefore, the derivatives of $\ln l_1(u)$ and $\ln l_2(u)$ have Fourier transforms. Taking logarithms and derivatives of both sides of (4.14), and then Fourier transforms, we find that

$$
\begin{aligned}
&[\ln l_1(u)]' = \frac{1}{2\pi \mathrm{i}} \int_{\mathrm{Re}(v)=0} \mathrm{d}v [\ln p_2(v)]' 5/\sin 5(u-v) \\
&0 < \mathrm{Re}(u) < \min\{\pi/5, 3\pi/10 - u_0\} \\
&[\ln l_2(u)]' = \frac{1}{2\pi \mathrm{i}} \int_{\mathrm{Re}(v)=\pi/2} \mathrm{d}v [\ln p_1(v)]' 5/\sin 5(u-v) \\
&\pi/2 < \mathrm{Re}(u) < 7\pi/10 - u_0 .
\end{aligned}
\tag{4.16}
$$

We integrate (4.16) with integration constants D_1 and D_2 as

$$
\begin{aligned}
\ln \alpha(x) &= k * \ln \bar{\beta}(x) + D_1 \\
\ln \bar{\alpha}(x) &= \ln Z\left[(x/5)\mathrm{i} + (3\pi/5)\right] + k * \ln \beta(x) + D_2
\end{aligned}
\tag{4.17}
$$

where

$$
\begin{aligned}
\alpha(x) &= \beta(x) - 1 = T_1\left[(x/5)\mathrm{i} + (\pi/10)\right] \\
\bar{\alpha}(x) &= \bar{\beta}(x) - 1 = T_1\left[(x/5)\mathrm{i} + (6\pi/10)\right]
\end{aligned}
\tag{4.18}
$$

and $f * g(x)$ is the convolution of the functions $f(x)$ and $g(x)$:

$$
f * g(x) = \int_{-\infty}^{\infty} g(x-y) f(y)\, \mathrm{d}y . \tag{4.19}
$$

The kernel $k(x)$ is given by

$$
k(x) = 1/2\pi \cosh(x) . \tag{4.20}
$$

Take the $x \to \pm\infty$ limit in (4.17). Then, from (c), it follows that

$$
D_1 = D_2 = 0 . \tag{4.21}
$$

The equation (4.17) with (4.21) is exact, even for finite l.

Now we investigate the asymptotic behaviour of $T_1(u)$ as l becomes large. Noting the property (b), we define the following functions:

$$
\begin{aligned}
a_\pm(x) =& A_\pm(x) - 1 = \lim_{l\to\infty} \alpha(\pm x \pm \ln l) \\
\bar{a}_\pm(x) =& \bar{A}_\pm(x) - 1 = \lim_{l\to\infty} \bar{\alpha}(\pm x \pm \ln l) .
\end{aligned}
\tag{4.22}
$$

From (4.17) it is shown that the functions $a_\pm(x)$, $\bar{a}_\pm(x)$ satisfy the equations

$$\begin{aligned}\ln a_\pm(x) &= k * \ln \bar{A}_\pm(x)\\ \ln \bar{a}_\pm(x) &= -2\mathrm{e}^{-x}(m + n\mathrm{e}^{\pm 5\mathrm{i}u_0}) + k * \ln A_\pm(x)\,.\end{aligned} \tag{4.23}$$

For large l, the first equation of (4.17) is rewritten by the use of $\bar{A}_\pm(x)$ as

$$\ln T_1(u) \sim \frac{1}{\pi l}\left[\mathrm{e}^x \int_\infty^\infty \mathrm{d}y\, \mathrm{e}^{-y} \ln \bar{A}_+(y) + \mathrm{e}^{-x} \int_\infty^\infty \mathrm{d}y\, \mathrm{e}^{-y} \ln \bar{A}_-(y)\right] \tag{4.24}$$

with $u = (x/5)\mathrm{i} + \pi/10$. From (4.23) it follows that

$$\begin{aligned}2\big(m + n\mathrm{e}^{\pm 5\mathrm{i}u_0}\big) &\int_{-\infty}^{\infty} \mathrm{d}x\, \mathrm{e}^{-x} \left\{\ln \bar{A}_\pm(x) + [\ln \bar{A}_\pm(x)]'\right\}\\ &= \int_{-\infty}^{\infty} \mathrm{d}x \left\{[\ln a_\pm(x)]' \ln A_\pm(x) - \ln a_\pm(x)[\ln A_\pm(x)]'\right\}\\ &\quad + \int_{-\infty}^{\infty} \mathrm{d}x \left\{[\ln \bar{a}_\pm(x)]' \ln \bar{A}_\pm(x) - \ln \bar{a}_\pm(x)[\ln \bar{A}_\pm(x)]'\right\}\,.\end{aligned} \tag{4.25}$$

Integrating the LHS by parts and using (4.22) in the RHS gives

$$\begin{aligned}4\big(m + n\mathrm{e}^{\pm 5\mathrm{i}u_0}\big) &\int_{-\infty}^{\infty} \mathrm{d}x\, \mathrm{e}^{-x} \ln \bar{A}_\pm(x)\\ &= \int_{a_\pm(-\infty)}^{a_\pm(\infty)} \mathrm{d}a_\pm [a_\pm^{-1} \ln(1 + a_\pm) - (1 + a_\pm)^{-1} \ln a_\pm]\\ &\quad + \int_{\bar{a}_\pm(-\infty)}^{\bar{a}_\pm(\infty)} \mathrm{d}\bar{a}_\pm [\bar{a}_\pm^{-1} \ln(1 + \bar{a}_\pm) - (1 + \bar{a}_\pm)^{-1} \ln \bar{a}_\pm]\,.\end{aligned} \tag{4.26}$$

From (c) and (4.23), we deduce that

$$\begin{aligned}a_\pm(-\infty) &= 1 \qquad & a_\pm(\infty) &= (1 + \sqrt{5})/2\\ \bar{a}_\pm(-\infty) &= 0 \qquad & \bar{a}_\pm(\infty) &= (1 + \sqrt{5})/2\,.\end{aligned} \tag{4.27}$$

Substituting (4.27) into (4.26), we get

$$\begin{aligned}4\big(m + n\mathrm{e}^{\pm 5\mathrm{i}u_0}\big) &\int_{-\infty}^{\infty} \mathrm{d}x\, \mathrm{e}^{-x} \ln \bar{A}_\pm(x) = 4L_+\big[(\sqrt{5} + 1)/2\big] - 2L_+(1)\\ &= 4L\big[\big(\sqrt{5} - 1\big)/2\big] - 2L(1/2) = 7\pi^2/30\end{aligned} \tag{4.28}$$

where $L_+(u)$ is a dilogarithmic function defined by

$$L_+(a) = \frac{1}{2}\int_0^a \left[\frac{\ln(1 + b)}{b} - \frac{\ln b}{1 + b}\right] \tag{4.29}$$

and $L(a)$ is the Rogers dilogarithm

$$L(a) = -\frac{1}{2}\int_0^a \left[\frac{\ln(1 - b)}{b} + \frac{\ln b}{1 - b}\right]. \tag{4.30}$$

The dilogarithm $L_+(a)$ is related to the Rogers dilogarithm as

$$L_+(a) = L[x/(1+x)]\,. \tag{4.31}$$

(For detailed definitions of the dilogarithmic functions and relations among them, see the appendix in KP and [30].) Using (4.28) in (4.24), and after some calculations, we find that for u in strip 1

$$\ln T_1(u) \sim \frac{1}{\pi N}\frac{7\pi^2}{120}\left[\frac{\mathrm{e}^x}{\tan\varphi + \mathrm{e}^{5\mathrm{i}u_0}} + \frac{\mathrm{e}^{-x}}{\tan\varphi + \mathrm{e}^{-5\mathrm{i}u_0}}\right] \tag{4.32a}$$

with $u = (x/5)\mathrm{i} + \pi/10$.

For finite-size corrections of other eigenvalues, the arguments in sections 2.2–2.5 of KP are repeated with some modifications. We obtain the following results: for u in strip 1

$$\ln T_2(u) \sim \pi\mathrm{i} - \frac{\pi}{60N}\left[\frac{\mathrm{e}^x}{\tan\varphi + \mathrm{e}^{5\mathrm{i}u_0}} + \frac{\mathrm{e}^{-x}}{\tan\varphi + \mathrm{e}^{-5\mathrm{i}u_0}}\right] \tag{4.32b}$$

$$\ln T_{3;k_+,k_-}(u) \sim \frac{\pi}{N}\left[\frac{\mathrm{e}^x}{\tan\varphi + \mathrm{e}^{5\mathrm{i}u_0}}\left(-2k_+ - \tfrac{17}{120}\right) + \frac{\mathrm{e}^{-x}}{\tan\varphi + \mathrm{e}^{-5\mathrm{i}u_0}}\left(-2k_- - \tfrac{17}{120}\right)\right] \tag{4.32c}$$

$$\ln T_{4;k_+,k_-}(u) \sim \pi\mathrm{i} + \frac{\pi}{N}\left[\frac{\mathrm{e}^x}{\tan\varphi + \mathrm{e}^{5\mathrm{i}u_0}}\left(-2k_+ - \tfrac{49}{60}\right) + \frac{\mathrm{e}^{-x}}{\tan\varphi + \mathrm{e}^{-5\mathrm{i}u_0}}\left(-2k_- - \tfrac{49}{60}\right)\right] \tag{4.32d}$$

$$\ln T_{5;k_+,k_-}(u) \sim \frac{\pi}{N}\left[\frac{\mathrm{e}^x}{\tan\varphi + \mathrm{e}^{5\mathrm{i}u_0}}\left(-2k_+ - \tfrac{137}{120}\right) + \frac{\mathrm{e}^{-x}}{\tan\varphi + \mathrm{e}^{-5\mathrm{i}u_0}}\left(-2k_- - \tfrac{137}{120}\right)\right] \tag{4.32e}$$

$$\vdots$$

with $u = (x/5)\mathrm{i} + \pi/10$. In (4.32$c$–$e$) we represent the jth eigenvalue and its descendants as $T_{j;k_+,k_-}(u)$ with $k_\pm = 0, 1, 2, \ldots$.

4.2. *Critical hard hexagons*

In the case of critical hard hexagons we suppose that $-\lambda < u_0 < 0$. We also assumed that $M + N \equiv 0 \pmod 3$. The eigenvalues $T(u)$ are calculated in a similar way to the previous subsection. Our attention is restricted to the largest eigenvalues in the strips $-\lambda - u_0 < \mathrm{Re}(u) < 0$ and $\lambda - u_0 < \mathrm{Re}(u) < 2\lambda$.

Firstly, we determine the bulk behaviour of $T(u)$ by considering a transfer matrix $\mathbf{T}(u;x)$, which is given by (3.3) with the face weight (2.4) replaced by (3.14) in [24]. The eigenvalues of $\mathbf{T}(u;x)$ are denoted by $T(u;x)$. As $l \to \infty$ with m and n fixed to be constants, we find the asymptotic forms of $T(u;x)$, which are the largest in the strips $-\lambda - u_0 < \mathrm{Re}(u) < 0$ and $\lambda - u_0 < \mathrm{Re}(u) < 2\lambda$, by the same argument as [27]. From the calculated $T(u;x)$, it follows that

$$\begin{aligned}\lim_{l\to\infty} T(u)^{1/l} &= \lim_{x\to 1}\lim_{l\to\infty} T(u;x)^{1/l} \\ &= \begin{cases} Z_1(u) & \text{for } u \text{ in strip 1} \\ Z_2(u) & \text{for } u \text{ in strip 2} \end{cases}\end{aligned} \tag{4.33}$$

where

$$\begin{aligned} Z_1(u) &= z(u)^m z(u+u_0)^n \\ Z_2(u) &= 1/z(u-\pi/5)^m z(u+u_0-\pi/5)^n \end{aligned} \tag{4.34}$$

with

$$z(u) = \sin(5u/3 - \pi/3)/\sin(5u/3 + \pi/3) \tag{4.35}$$

and the two strips are defined by

$$\begin{aligned} &\text{strip 1:} \quad -2\pi/5 - u_0 < \mathrm{Re}(u) < \pi/10 \\ &\text{strip 2:} \quad \pi/10 - u_0 < \mathrm{Re}(u) < 3\pi/5\,. \end{aligned} \tag{4.36}$$

Secondly, we repeat almost the same analyses in KP to find integral equations for finite-size corrections of $T(u)$. The argument in section 3.1 of KP is applied to the largest eigenvalue $T_1(u)$. After some calculations, we obtain for u in strip 1

$$\ln T_1(u) \sim l \ln Z_1(u) + \frac{\pi}{15N}\left[\frac{\mathrm{e}^x}{\tan\varphi + \mathrm{e}^{10\mathrm{i}u_0/3}} + \frac{\mathrm{e}^{-x}}{\tan\varphi + \mathrm{e}^{-10\mathrm{i}u_0/3}}\right] \tag{4.37a}$$

with $u = (3x/10)\mathrm{i} - (3\pi/20)$; for u in strip 2, $\ln Z_1(u)$ is replaced by $\ln Z_2(u)$ in the RHS and $u = (3x/10)\mathrm{i} + (7\pi/20)$.

A doublet of the next-largest eigenvalues $T_2^{(\pm)}(u)$ are determined. The argument in section 3.2 of KP shows that for u in strip 1

$$\ln T_2^{(+)}(u) \sim l \ln Z_1(u) + 2\pi\mathrm{i}/3 - \frac{\pi}{15N}\left[\frac{\mathrm{e}^x}{\tan\varphi + \mathrm{e}^{10\mathrm{i}u_0/3}} + \frac{\mathrm{e}^{-x}}{\tan\varphi + \mathrm{e}^{-10\mathrm{i}u_0/3}}\right] \tag{4.37b}$$

with $u = (3x/10)\mathrm{i} - (3\pi/20)$; replacing $\ln Z_1(u)$ and $+2\pi\mathrm{i}/3$ by $\ln Z_2(u)$ and $-2\pi\mathrm{i}/3$ in the RHS, respectively, gives the expression for u in strip 2 with $u = (3x/10)\mathrm{i} + (7\pi/20)$. The other next-largest eigenvalue $T_2^{(-)}(u)$ is the complex conjugate of $T_2^{(+)}(u)$. (Hereafter, we represent by $T^{(\pm)}(u)$ a doublet of eigenvalues which are complex conjugates.)

Analysis for the next-next-largest eigenvalue $T_3(u)$ is somewhat complicated. According to the locations of the zeros u_j, we move the paths of Fourier integrals. When $m/n = 1$, for example, numerical analyses for finite-size systems show that, in a periodic strip $-2\pi/5 < \mathrm{Re}(u) < 3\pi/5$ and for sufficient large l, the zeros u_j appear near the lines $\mathrm{Re}(u) = -2\pi/5 - u_0/2$ and $\mathrm{Re}(u) = \pi/10 - u_0/2$ densely except four zeros $u_{1\pm}$ and $u_{2\pm}$. Noting that the zeros $u_{1\pm}$ are close to the line $\mathrm{Re}(u) = -\pi/5 - u_0/2$, and $u_{2\pm}$ the line $\mathrm{Re}(u) = 2\pi/5 - u_0/2$, we move the path of each Fourier integral in (3.8) and (3.9) of KP by $-u_0/2$ along the real axis. Then, from almost the same analysis in section 3.3 of KP, it follows that for u in strip 1:

$$\begin{aligned} \ln T_{3;k_+,k_-}(u) \sim l \ln Z_1(u) - 2\pi\mathrm{i} + \frac{\pi}{N}\bigg[&\frac{\mathrm{e}^x}{\tan\varphi + \mathrm{e}^{10\mathrm{i}u_0/3}}\left(-4k_+ - \tfrac{11}{15}\right) \\ &+ \frac{\mathrm{e}^{-x}}{\tan\varphi + \mathrm{e}^{-10\mathrm{i}u_0/3}}\left(-4k_- - \tfrac{11}{15}\right)\bigg] \end{aligned} \tag{4.37c}$$

with $u = (3x/10)\mathrm{i} - (3\pi/20)$; $\ln Z_1(u)$ (respectively $-2\pi\mathrm{i}$) is replaced by $\ln Z_2(u)$ (respectively $2\pi\mathrm{i}$) and $u = (3x/10)\mathrm{i} + (7\pi/20)$ for u in strip 2. We denote the next-next-largest eigenvalue and its descendants by $T_{3;k_+,k_-}(u)$ with $k_\pm = 0, 1, 2, \ldots$.

Similarly to the analysis for $T_{3;k_+,k_-}(u)$, we repeat the arguments in sections 3.4–3.6 of KP with some modifications, including movements of paths of Fourier integrals. We find that for u in strip 1

$$\ln T^{(+)}_{4;k}(u) \sim l \ln Z_1(u) + 4\pi\mathrm{i}/3 + \frac{\pi}{N}\left[\frac{\mathrm{e}^{x}}{\tan\varphi + \mathrm{e}^{10\mathrm{i}u_0/3}}\left(-4k - \tfrac{31}{15}\right) + \frac{\mathrm{e}^{-x}}{\tan\varphi + \mathrm{e}^{-10\mathrm{i}u_0/3}}\left(-\tfrac{1}{15}\right)\right] \tag{4.37d}$$

$$\ln T^{(+)}_{5;k_+,k_-}(u) \sim l \ln Z_1(u) + 2\pi\mathrm{i}/3 + \frac{\pi}{N}\left[\frac{\mathrm{e}^{x}}{\tan\varphi + \mathrm{e}^{10\mathrm{i}u_0/3}}\left(-4k_+ - \tfrac{19}{15}\right) + \frac{\mathrm{e}^{-x}}{\tan\varphi + \mathrm{e}^{-10\mathrm{i}u_0/3}}\left(-4k_- - \tfrac{19}{15}\right)\right] \tag{4.37e}$$

$$\ln T^{(+)}_{6;k_+,k_-}(u) \sim l \ln Z_1(u) + \frac{\pi}{N}\left[\frac{\mathrm{e}^{x}}{\tan\varphi + \mathrm{e}^{10\mathrm{i}u_0/3}}\left(-4k_+ - \tfrac{31}{15}\right) + \frac{\mathrm{e}^{-x}}{\tan\varphi + \mathrm{e}^{-10\mathrm{i}u_0/3}}\left(-4k_- - \tfrac{11}{15}\right)\right] \tag{4.37f}$$

with $u = (3x/10)\mathrm{i} - (3\pi/20)$ and $k_{(\pm)} = 0, 1, 2, \ldots$; for u in strip 2 $\ln Z_1(u)$ (respectively $+4\pi\mathrm{i}/3$ in (3.47*d*), $+2\pi\mathrm{i}/3$ in (3.47*e*)) is replaced by $\ln Z_2(u)$ (respectively $-4\pi\mathrm{i}/3$, $-2\pi\mathrm{i}/3$) and $u = (3x/10)\mathrm{i} + (7\pi/20)$. We also find the conjugate eigenvalues $T^{(-)}_{4;k}(u)$, $T^{(-)}_{5;k_+,k_-}(u)$, and $T^{(-)}_{6;k_+,k_-}(u)$.

5. Spatial anisotropy and conformal invariance

Now, substituting $T(u)$ determined in section 4 into (3.8), we investigate the partition function Ξ. Emphases are placed on its finite-size correction Ξ_c [14, 15], which is defined by

$$\Xi_c = \lim_{l,l'\to\infty} \Xi/\kappa^{ll'} \tag{5.1}$$

where the limit is taken with the ratio $\delta = l'/l$ fixed to be a constant and κ is

$$\kappa = \lim_{l,l'\to\infty} \Xi^{1/ll'} = \lim_{l\to\infty} V_1(u_0)^{1/l}. \tag{5.2}$$

For tricritical hard squares it is supposed that $M + N \equiv M' + N' \equiv 0 \pmod 2$. We set $u = 0$ and $\lambda - u_0$ in (4.32). Substituting the eigenvalues $T(0)$ and $T(\lambda - u_0)$ into (3.8), we find that [31]

$$\ln\left[V_1(u_0)/\kappa^{l}\right]^{l'} \sim (\pi/6)(l'/l)(7/10)/\Gamma^2 \tag{5.3a}$$

$$\ln\left[V_2(u_0)/V_1(u_0)\right]^{l'} \sim (M'+N')\pi\mathrm{i} - 2\pi(l'/l)(3/40)/\Gamma^2 \tag{5.3b}$$

$$\ln\left[\frac{V_{3;k_+,k_-}(u_0)}{V_1(u_0)}\right]^{l'} \sim -2\pi\frac{l'}{l}\left(k_+ + k_- + \tfrac{1}{5}\right)\frac{1}{\Gamma^2} + 2\pi\mathrm{i}\frac{l'}{l}(k_+ - k_-)\frac{\Delta}{\Gamma^2} \tag{5.3c}$$

$$\ln\left[\frac{V_{4;k_+,k_-}(u_0)}{V_1(u_0)}\right]^{l'} \sim (M'+N')\pi\mathrm{i} - 2\pi\frac{l'}{l}\left(k_+ + k_- + \tfrac{7}{8}\right)\frac{1}{\Gamma^2} + 2\pi\mathrm{i}\frac{l'}{l}(k_+ - k_-)\frac{\Delta}{\Gamma^2} \tag{5.3d}$$

$$\ln\left[\frac{V_{5;k_+,k_-}(u_0)}{V_1(u_0)}\right]^{l'} \sim -2\pi\frac{l'}{l}\left(k_+ + k_- + \tfrac{6}{5}\right)\frac{1}{\Gamma^2} + 2\pi\mathrm{i}\frac{l'}{l}(k_+ - k_-)\frac{\Delta}{\Gamma^2} \tag{5.3e}$$

where $k_\pm = 0, 1, 2, \ldots$ and

$$\begin{aligned}\Delta &= \left(\gamma^2 - \gamma^{-2}\right)\sin\theta\cos\theta \\ \Gamma^2 &= \gamma^2\cos^2\theta + \gamma^{-2}\sin^2\theta\end{aligned} \tag{5.4}$$

with

$$\begin{aligned}\gamma^2 &= \tan(\pi u_0/2\lambda) \\ \theta &= \varphi + \pi/4\,.\end{aligned} \tag{5.5}$$

We consider the case of isotropic interactions $u_0 = \lambda/2$. From (5.5) it follows that $\gamma^2 = 1$. Substituting $\gamma^2 = 1$ into (5.4) gives $\Delta = 0$ and $\Gamma = 1$. If $l' \gg l \gg 1$, after Ξ_c is expanded as (3.8*a*), we use (5.3) in the expansion. It is found that, within the validity of the expansion, Ξ_c is a function of the ratio l'/l but is independent of the rotation angle θ. The result shows that the system is invariant under scale transformations and rotations. We also know that the system is invariant under translations. Though the global transformations cannot be generalized to local ones directly, it is suggested that the system is conformally invariant. As shown in KP, the eigenvalue spectrum is in agreement with (4.6), which is generated by the modular invariant partition function $Z_c^{(\mathrm{sq})}(q)$. We identify Ξ_c with $Z_c^{(\mathrm{sq})}$. If we consider anisotropic systems, τ in (4.3*b*) is replaced by

$$\tau = (l'/l)(\mathrm{i}+\Delta)/\Gamma^2\,. \tag{5.6}$$

For critical hard hexagons we assume that $M+N \equiv M'-N' \equiv 0 \pmod 3$. Substituting (4.37) into (3.8) with $u = 0$ and $\lambda - u_0$, we get

$$\ln\left[V_1(u_0)/\kappa^l\right]^{l'} \sim (\pi/6)(l'/l)\left(\tfrac{4}{5}\right)/\Gamma^2 \tag{5.7a}$$

$$\ln\left[V_2^{(\pm)}(u_0)/V_1(u_0)\right]^{l'} \sim \pm(M'-N')2\pi\mathrm{i}/3 - 2\pi(l'/l)\left(\tfrac{2}{15}\right)/\Gamma^2 \tag{5.7b}$$

$$\ln\left[\frac{V_{3;k_+,k_-}(u_0)}{V_1(u_0)}\right]^{l'} \sim -2\pi\frac{l'}{l}\left(2k_+ + 2k_- + \tfrac{4}{5}\right)\frac{1}{\Gamma^2} - 2\pi\mathrm{i}\frac{l'}{l}(2k_+ - 2k_-)\frac{\Delta}{\Gamma^2} \tag{5.7c}$$

$$\ln\left[\frac{V^{(\pm)}_{4;k_+,k_-}(u_0)}{V_1(u_0)}\right]^{l'} \sim \pm(M'-N')\frac{4\pi}{3}\mathrm{i} - 2\pi\frac{l'}{l}\left(2k - \tfrac{13}{15}\right)\frac{1}{\Gamma^2} \mp 2\pi\mathrm{i}\frac{l'}{l}(2k-1)\frac{\Delta}{\Gamma^2} \tag{5.7d}$$

$$\ln\left[\frac{V^{(\pm)}_{5;k_+,k_-}(u_0)}{V_1(u_0)}\right]^{l'} \sim \pm(M'-N')\frac{2\pi}{3}\mathrm{i} - 2\pi\frac{l'}{l}\left(2k_+ + 2k_- - \tfrac{8}{3}\right)\frac{1}{\Gamma^2} \mp 2\pi\mathrm{i}\frac{l'}{l}(2k_+ - 2k_-)\frac{\Delta}{\Gamma^2} \tag{5.7e}$$

$$\ln\left[\frac{V^{(\pm)}_{6;k_+,k_-}(u_0)}{V_1(u_0)}\right]^{l'} \sim -2\pi\frac{l'}{l}\left(2k_+ + 2k_- - \tfrac{1}{5}\right)\frac{1}{\Gamma^2} \mp 2\pi\mathrm{i}\frac{l'}{l}(2k_+ - 2k_- - 1)\frac{\Delta}{\Gamma^2} \tag{5.7f}$$

$$\vdots$$

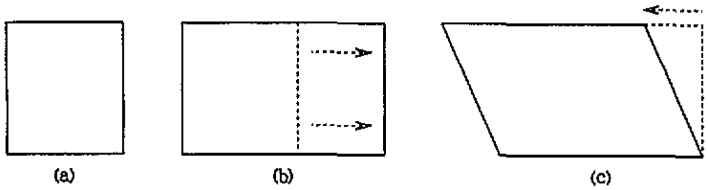

Figure 3. For most anisotropic systems conformal invariance is restored by deforming the geometry of the lattice.

where $k_{(\pm)} = 0, 1, 2, \ldots$. The eigenvalue spectrum agrees with (4.8) if τ is redefined by (5.4) and (5.6) with γ^2 replaced by

$$\gamma^2 = -\tan(\pi u_0/3\lambda)\,. \tag{5.8}$$

For given values of u_0 and θ, (5.6) shows that the anisotropic system has the same finite-size correction Ξ_c as the conformal invariant one if the geometry of the anisotropic system is deformed as follows (figure 3): stretch the original lattice along either of the two coordinate axes ($\tau \to \tau\Gamma^2$), shear it into a parallelogram ($\tau \to \tau - \Delta l'/l$), and then impose on it toroidal boundary conditions. The deformation corresponds to an anisotropic rescaling of length by amount of γ^2 along a direction rotated through θ from the coordinate axes. Note that γ^2 is independent of θ. It is suggested that conformal invariance of the system is restored by the anisotropic rescaling. We consider the case $u_0 = -\lambda$, for example. In this limit the model reduces to the hard-hexagon model. Substituting $u_0 = -\lambda$ into (5.8) shows that

$$\gamma^2 = \sqrt{3}\,. \tag{5.9}$$

By the anisotropic rescaling the square lattice is deformed into a triangular one. We define a shift operator $\mathbf{S}$ by

$$\mathbf{S} = \left[\mathbf{T}(0)^m \mathbf{T}(-u_0)^n\right]^{l''} \tag{5.10}$$

with $(m+n)l'' \equiv 0 \pmod 3$. Returning to the inhomogeneous system (3.1), and introducing the shift operator $\mathbf{S}$ into (3.1), we can investigate the triangular lattice and its rotations. Then, we find scale and rotational invariance of finite-size correction Ξ_c of the hard-hexagon model, as shown in the case of isotropic tricritical hard squares.

Finally, we fix the rotation angle to be $\theta = \varphi + \pi/4 = \pi/2$ with $m = n = 1$ and consider one-dimensional quantum systems associated with tricritical hard squares and critical hard hexagons [1, 4, 18, 21, 32]. From (5.4)–(5.6), and (5.8) it follows that

$$\tau = \mathrm{i}(l'/l)\gamma^2 \tag{5.11}$$

with

$$\gamma^2 = \begin{cases} \tan(\pi u_0/2\lambda) & \text{for tricritical hard squares} \\ -\tan(\pi u_0/3\lambda) & \text{for critical hard hexagons}\,. \end{cases} \tag{5.12}$$

Equations (2.6) and (2.6′) show that

$$\lim_{u_0 \to 0} \mathbf{V}(u_0) = \mathbf{I} \tag{5.13}$$

with the identity matrix $\mathbf{I}$. Hamiltonians H of one-dimensional quantum systems of $2l$ sites are defined by

$$\mathbf{V}(\delta u_0) = \mathbf{I} - \delta u_0 H + \cdots \qquad \delta u_0 \sim 0\,. \tag{5.14}$$

Quantum system I is associated with tricritical hard squares, and II critical hard hexagons. Finite-size corrections of the partition functions of the quantum systems, denoted by $\bar{\Xi}_c$, are obtained as

$$\bar{\Xi}_c = \lim_{l'\to\infty} \Xi_c = Z_c(\bar{q}) \tag{5.15}$$

where the limit is taken with $u_0 = \pm\beta/l'$; the upper sign is for the quantum system I, and the lower sign for the quantum system II; β is the inverse temperature and

$$\begin{aligned} \bar{q} &= \exp 2\pi\mathrm{i}\bar{\tau} \\ \bar{\tau} &= \lim_{l'\to\infty} \mathrm{i}(l'/l)\tan(\beta\bar{v}/2l') = \mathrm{i}(\beta/2l)\bar{v}\,. \end{aligned} \tag{5.16}$$

Note that taking the limit has an role of replacing the ratio $\delta = l'/l$ of classical systems by the ratio $\bar{\delta} = \beta/2l$ of the quantum systems. The ratio $\bar{\delta}$ is multiplied by an anisotropy factor (or effective light velocity) $\bar{v}$ which is determined by the derivative of γ^2 at $u_0 = 0$ as

$$\bar{v} = \begin{cases} \pi/\lambda & \text{for quantum system I} \\ 2\pi/3\lambda & \text{for quantum system II}\,. \end{cases} \tag{5.17}$$

When $\beta \gg 2l \gg 1$, the leading behaviour of the free energy $\bar{F}$ of the quantum systems is

$$\bar{F} \sim 2l\beta\epsilon - (\beta/2l)\bar{v}(\pi c/6) + \cdots \tag{5.18}$$

where ϵ is the (per-site) ground state energy determined by

$$\begin{aligned} \epsilon &= -\frac{1}{2}\frac{\mathrm{d}\kappa}{\mathrm{d}u_0}\bigg|_{u_0=0} \\ &= \begin{cases} 0 & \text{for quantum system I} \\ 10/3\sqrt{3} & \text{for quantum system II} \end{cases} \end{aligned} \tag{5.19}$$

and the second term is a universal one containing the central charge c; for quantum system I (or II) $c = \frac{7}{10}$ $\left(\text{or } \frac{4}{5}\right)$.

To consider $\bar{F}$ for $2l \gg \beta \gg 1$, it is convenient to see the lattice from a $\pi/2$ rotated frame [32]. This is achieved by changing the parameter u_0 into $\lambda - u_0$. In (5.11) γ^2 is replaced by

$$\gamma^2 = \begin{cases} \cot(\pi u_0/2\lambda) & \text{for tricritical hard squares} \\ -\cot(\pi u_0/3\lambda) & \text{for critical hard hexagons}\,. \end{cases} \tag{5.20}$$

Finite-size corrections $\bar{\Xi}_c$ of the quantum systems of $2l'$ sites are calculated as

$$\bar{\Xi}_c = \lim_{l\to\infty} \Xi_c|_{u_0=\pm\beta/l} = Z_c(\bar{q}) \tag{5.21}$$

with

$$\begin{aligned} \bar{q} &= \exp 2\pi\mathrm{i}\bar{\tau} \\ \bar{\tau} &= \lim_{l\to\infty} \mathrm{i}(l'/l)\cot(\beta\bar{v}/2l) = \mathrm{i}(2l'/\beta)(1/\bar{v})\,. \end{aligned} \tag{5.22}$$

Supposing that $2l' \gg \beta \gg 1$, we obtain [33]

$$\bar{F} \sim 2l'\beta\epsilon - (2l'/\beta)(1/\bar{v})(\pi c/6) + \cdots\,. \tag{5.23}$$

The second term in the RHS of (5.23) is also found from (5.15) by the use of the invariance of Z_c under the modular transformation $\bar{\tau} \to -1/\bar{\tau}$.

6. Summary and discussion

In this paper we considered a square lattice rotated through an arbitrary angle φ with respect to the coordinate axes. Then, a method was developed to analyse solvable models on it. In the method we used three properties of the face weights: the Yang–Baxter relation, the standard initial condition, and the crossing symmetry. Auxiliary faces were introduced into a rotated system to relate it with an inhomogeneous one in the natural orientation. The inhomogeneous system was analysed by commuting a transfer matrix argument.

By the new method we investigated tricritical hard squares and critical hard hexagons. Supposing the models on a torus of size $l \times l'$, we considered expansions of finite-size corrections Ξ_c of the partition functions by the use of some largest eigenvalues of transfer matrices. In the case of isotropic tricritical hard squares it was found that the expansion is a function of the ratio l'/l but is independent of the rotation angle φ, which shows invariance of the system under scale transformations and rotations. The scale and rotational invariance gives an evidence for conformal invariance.

For most anisotropic systems extra factors Γ^2 and Δ appeared in the expansion of Ξ_c, which showed that the rotational invariance of the system is broken. Representing Γ^2 and Δ as functions of φ, we found that the rotational invariance is restored by a suitable anisotropic rescaling of length by γ^2; if the lattice is rotated through φ with respect to the coordinate axes, the direction along which the system is rescaled is rotated through $\theta = \varphi + \pi/4$; an important thing here is that γ^2 is independent of θ. The amount of rescaling γ^2 and its direction θ correspond to a ratio between major and minor axes and their orientation of an ellipse to which equilibrium crystal shapes in [34] reduce in the critical limit. We also find that γ^2 is in agreement with approaches from off-critical calculations in [35].

We considered the DDTMs of tricritical hard squares and critical hard hexagons. One-dimensional quantum systems were defined in the $u_0 \to 0$ or λ limit of DDTMs. We found that, if γ^2 is represented as a function of the spectral parameter u_0 and the crossing parameter λ, finite-size properties of the quantum system are directly derived from those of tricritical hard squares or critical hard hexagons through the function. We expect that the structure is a quite general one. As mentioned in section 1, the auxiliary faces method can be applied to a wide class of solvable models. We hope that this fact will be clarified in further publications.

It is known that a special class of the kagomé lattice eight-vertex model is solvable [1, 36]. The solvable class of the kagomé lattice eight-vertex model can be investigated by a combination of inhomogeneous RRTMs and a DDTM. It is shown that the auxiliary faces method is easily applicable to these problems. We will report detailed calculations elsewhere.

Acknowledgments

I wish to thank Professor Y Akutsu for his continuous encouragement and useful advice about the auxiliary faces method. I also thank the Special Researchers' Basic Science Program, RIKEN. This work was supported in part by the Research Aid of Inoue Foundation for Science.

References

[1] Baxter R J 1982 *Exactly Solved Models in Statistical Mechanics* (London: Academic)

[2] McCoy B M and Wu T T 1973 *The Two-Dimensional Ising Model* (Cambridge, MA: Harvard University Press)

[3] Wadati M, Deguchi T and Akutsu Y 1989 *Phys. Rep.* **180** 247–332

[4] Wadati M and Akutsu Y 1988 *Prog. Theor. Phys. Suppl.* **94** 1–41

[5] Sutherland B 1970 *J. Math. Phys.* **11** 3183–6

[6] Temperly H N V and Lieb E H 1971 *Proc. R. Soc.* A **322** 251–80

[7] Lieb H E and Wu F Y 1972 *Phase Transitions and Critical Phenomena* vol 1 ed C Domb and M S Green (London: Academic)

[8] Pegg N E 1978 *Ann. Israel Phys. Soc.* **2** 637–40
Bariev R Z 1982 *Theor. Math. Phys.* **49** 1021–8
Truong T T and Schotte K D 1983 *Nucl. Phys.* B **220** 77–101

[9] Litvin A A and Priezzhev V B 1990 *J. Stat. Phys.* **60** 307–21

[10] Lieb E H 1967 *Phys. Rev. Lett.* **18** 692–4; 1967 *Phys. Rev.* **162** 162–72

[11] Pfeuty P and Toulouse G 1975 *Introduction to the Renormalization Group and to Critical Phenomena* (New York: Wiley)

[12] Belavin A A, Polyakov A M and Zamolodchikov A B 1984 *J. Stat. Phys.* **34** 763–74; 1984 *Nucl. Phys.* B **241** 333–80

[13] Cardy J L 1987 *Phase Transitions and Critical Phenomena* vol 11 ed C Domb and J L Lebowitz (London: Academic)

[14] Itzykson C and Drouffe J M 1989 *Statistical Field Theory* (Cambridge: Cambridge University Press) ch 9

[15] Cardy J L 1986 *Nucl. Phys.* B **270** 186–204

[16] Blöte H W, Cardy J L and Nightingale M P 1986 *Phys. Rev. Lett.* **56** 742–5

[17] Harmer C J 1985 *J. Phys. A: Math. Gen.* **18** L1133–7; 1986 *J. Phys. A: Math. Gen.* **19** 3335–51
de Vega H J and Woynarovich F 1985 *Nucl. Phys.* B **251** 439–56

[18] Bazhanov V V and Reshetikhin N Y 1989 *Int. J. Mod. Phys.* A **4** 115–42

[19] P A Pearce and A Klümper 1991 *Phys. Rev. Lett.* **66** 974–7

[20] Klümper A and Pearce P A 1991 *J. Stat. Phys.* **64** 13–76

[21] Klümper A 1992 *Ann. Phys., NY* **1** 540–53

[22] Klümper A, Wehner T and Zittartz J 1993 *J. Phys. A: Math. Gen.* **26** 2815–27

[23] Baxter R J 1980 *J. Phys. A: Math. Gen.* **13** L61–L70; 1981 *J. Stat. Phys.* **26** 427–52

[24] Baxter R J and Pearce P A 1982 *J. Phys. A: Math. Gen.* **15** 897–910

[25] Baxter R J and Pearce P A 1983 *J. Phys. A: Math. Gen.* **16** 2239–55

[26] Huse D A 1982 *Phys. Rev. Lett.* **49** 1121–4

[27] Fujimoto M 1990 *J. Stat. Phys.* **61** 1297–306

[28] Friedan D, Qiu Z and Shenker S 1984 *Phys. Rev. Lett.* **52** 1575–8

[29] Kac V G 1979 *Group Theoretical Methods in Physics (Lecture Notes in Physics 94)* ed W Beiglböck *et al* (Berlin: Springer)

[30] Lewin L 1958 *Dilogarithms and Associated Functions* (London: McDonald)

[31] Nightingale M P and Blöte H W 1983 *J. Phys. A: Math. Gen.* **16** L657–64

[32] Suzuki J, Akutsu Y and Wadati M 1990 *J. Phys. Soc. Japan* **59** 2667–80

[33] Affleck I 1986 *Phys. Rev. Lett.* **56** 746–8

[34] Fujimoto M 1993 *J. Phys. A: Math. Gen.* **26** 2285–99

[35] Kim D and Pearce P A 1987 *J. Phys. A: Math. Gen.* **20** L451–6

[36] Kwon K-H and Kim D *Preprint*